The EUMETSAT Satellite Application Facility on Land Surface Analysis

Algorithm Theoretical Basis Document for

Down-welling Longwave Flux (DSLF)

PRODUCTS: LSA-10 (MDSLF)

DOCUMENT SIGNATURE TABLE

	Name	Date	Signature
Prepared by :	I. Trigo, S. Freitas, C. Barroso, I. Monteiro, P. Viterbo		
Approved by :	Land SAF Project Manager (IM)		

DOCUMENTATION CHANGE RECORD

Issue / Revision	Date	Description:
Version 0.1	20/03/2009	Version to be presented to OR-3
Version 0.2	15/06/2009	Minor changes following suggestion made by EB

DISTRIBUTION LIST

Internal Consortium Distribution		
Organisation	Name	No. Copies
IM	Pedro Viterbo	
IM	Luís Pessanha	
IM	Isabel Trigo	
IDL	Carlos da Camara	
IM	Isabel Monteiro	
IM	Sandra Coelho	
IM	Carla Barroso	
IM	Pedro Diegues	
IM	Teresa Calado	
IM	Benvinda Barbosa	
IM	Ana Veloso	
IMK	Folke-S. Olesen	
IMK	Frank Goettsche	
IMK	Ewa Kabsch	
MF	Jean-Louis Roujean	
MF	Olivier Hautecoeu	
MF	Dominique Carrer	
RMI	Françoise Meulenberghs	
RMI	Arboleda Alirio	
RMI	Nicolas Ghilain	
FMI	Niilo Siljamo	
UV	Joaquin Melia	
UV	F. Javier García Haro	
UV/EOLAB	Fernando Camacho	
UV	Aleixander Verger	

External Distribution		
Organisation	Name	No. Copies
EUMETSAT	Frédéric Gasiglia	
EUMETSAT	Dominique Faucher	
EUMETSAT	Lorenzo Sarlo	
EUMETSAT	Lothar Schueller	
EDISOFT	Teresa Cardoso	
EDISOFT	Carlos Vicente	
EDISOFT	Cleber Balan	
SKYSOFT	Rui Alves	
SKYSOFT	João Canário	

Steering Group Distribution		
Nominated by:	**Name**	**No. Copies**
IM	Carlos Direitinho Tavares	
EUMETSAT	Lorenzo Sarlo	
EUMETSAT	Yves Govaerts	
EUMETSAT	François Montagner	
STG/AFG (USAM)	Luigi de Leonibus	
MF	François Bouyssel	
RMI	Steven Dewitte	
FMI	Carl Fortelius	

Table of Contents

List of Tables

List of Figures

1. Introduction

The down-welling surface longwave flux (DSLF hereafter) is an important component of the heat exchange across the surface-atmosphere interface. Accurate values of DSLF are essential in determining the surface radiation budget, which controls to a large extent the surface energy balance (e.g., Kalma et al., 2008). Over large areas, DSLF is generally inferred from atmospheric models (e.g., Wild et al., 1995; Morcrette, 2002) or from satellite retrieved parameters (e.g., Gupta 1989, Gupta et al., 1992; Zhang et al., 1995; Diak et al., 2000). However, the modelling of surface radiation depends crucially on an accurate description of clouds. Model known deficiencies in the spatial and temporal representation of clouds (e.g., Crewell et al. 2002) may be overcome by satellite observations (Meetschen et al. 2004). Over the past 2 decades there has been a significant increase in the use of satellite data to identify clouds (e.g., Rossow and Garder, 1993; Feijt et al., 2000; Derrien and Gléau, 2005), as well as to retrieve top cloud properties (e.g, Gupta, 1989; Derrien and Gléau, 2005). Although cloud microphysics plays an important role in radiative processes within the cloud, both solar and thermal fluxes reaching the surface are largely determined by local cloud cover (e.g., Dürr and Philipona, 2004; Meetschen et al. 2004). Here we propose a methodology for the estimation of DSLF which combines the signature of clouds on infrared and visible channels with information on atmosphere water vapour content and near surface temperature from Numerical Weather Prediction (NWP) models. This is based on the assumption that the latter, which also include the assimilation of measurements from sounding instruments along with other remotely sensed and conventional observations, provide the best knowledge of atmospheric profiles at any given point.

Below we describe a bulk parameterization scheme to be applicable under all sky conditions. The adjustment of semi-empirical formulations to estimate DSLF from near surface data has been the subject of many studies before. Most of these are applicable for clear sky cases only, e.g., Brunt (1932), Idso and Jackson (1969), Brutsaert (1975), and more recently Prata (1996) and Dilley and O'Brien (1998). The limitation of these studies to clear conditions strongly limits their utility, however there have been fewer attempts have been made to derive all-sky parameterizations, e.g., Crawford and Duchon (1999), Diak et al., (2000) Josey et al. (2003), Bilbao and Miguel (2007). The formulation proposed here follows that first developed by Prata (1996) for clear sky cases, and now fine-tuned for a wider range of atmospheric conditions. The calibration of this semi-empirical method is based on downward infrared flux simulations obtained with the MODerate spectral resolution atmospheric TRANSmittance algorithm (MODTRAN4; Berk et al., 2000). The algorithm described here is the current baseline for the DSLF product, generated operationally by the EUMETSAT Satellite Application Facility on Land Surface Analysis (Land-SAF). It makes use of the cloud mask developed by the SAF on support to Nowcasting and Very Short-Range Forecasting for (NWC SAF; http://nwcsaf.inm.es/; Derrien and Gléau, 2005) to take advantage of the spectral characteristics of the Spinning Enhanced Visible and Infrared Imager (SEVIRI) onboard Meteosat (an identical approach is used for AVHRR/MetOp). Information on precipitable water and near surface air temperature is

obtained from forecasts of the European Centre for Medium-range Weather Forecasts (ECMWF). The validation of the new algorithm is performed against independent data through the comparison of DSLF estimates with in situ measurements. The validation exercise is extended to other bulk parameterizations for benchmarking and also to ECMWF flux forecasts, since the model is the main source of information on air temperature and water vapour content.

2. Downwelling Long-wave Flux at the Surface

2.1. Parameterization Schemes

Downwelling Surface Long-wave radiative Flux (DSLF) is defined as the total irradiance within infrared part of the spectrum (4-100 µm). Within this range atmospheric scattering may be neglected and DSLF corresponds essentially to radiation emitted by the lowest hundred meters of the atmosphere (Zhao et al., 1994). DSLF is often estimated as a bulk parameterization, where the thermal radiative flux reaching the surface is emitted by an atmospheric layer with emissivity ε_{sky}, and temperature T_{sky}:

$$F^{\downarrow} = \sigma \ \varepsilon_{sky} \ T_{sky}^4 \qquad (1)$$

where σ is the Stefan-Boltzmann constant. Amongst the greenhouse gases, water vapour is the most important contributor to DSLF, and also the most variable (e.g., Niemelä et al., 2004). Thus both ε_{sky} and T_{sky} are generally estimated as a function of near surface atmospheric temperature and/or water vapour content. Many of developed bulk parameterizations are applicable under clear sky conditions only. The presence of clouds contributes to a significant increase in DSLF, since they "close" the infrared atmospheric window (e.g., Takara and Ellingson, 2000). To take such effect into account, all-sky bulk parameterizations generally introduce correcting factors as a function of cloudiness estimated and, in some cases, of cloud base height (e.g., Gupta et al., 1992). Several formulations estimate cloud cover from the fraction between observed solar irradiance and that observed under clear skies (e.g., Crawford and Duchon, 1999; Bilbao and Miguel, 2007).

Several studies compared the performance of different methodologies (e.g., Prata, 1996; Crawford and Duchon, 1999; Niemelä et al., 2001; Bilbao and Miguel, 2007), but results are often inconclusive and highly dependent on the season and geographical location of the used for model verification. Table 1 summarizes the bulk parameterizations analysed in here, comprising two relatively recent schemes valid for clear sky conditions and one applicable for all situations.

Prata (1996) develops a clear sky emissivity model assuming a continuum absorption correction. Sky effective emissivity is a function of total column water vapour (see Table 1), while the sky effective temperature is the screen temperature;

model parameters were calibrated using in situ measurements. Here we will develop a similar formulation for DSLF, where ε_{sky} and T_{sky} in equation (1) are given by:

$$\varepsilon_{sky} = 1 - \left(1 + \frac{w}{10}\right)\exp\left(-\left(\alpha + \beta\frac{w}{10}\right)^m\right) \tag{2}$$

and

$$T_{sky} = T_o + \left(\gamma\Delta Td_o + \delta\right) \tag{3}$$

ε_{sky} is again a function of total column water vapour, w (mm), and T_{sky} equals 2m temperature, T_o (K), corrected by observed dew point depression at 2m (ΔTd_o). The parameters in equations (2) and (3), α, β, m, γ, and δ are fitted for clear sky and overcast conditions separately. We assume that for remote sensing retrievals, DSLF at the pixel scale results from the contribution of clear, $F_{clear}^{\downarrow}$, and cloudy, $F_{cloudy}^{\downarrow}$, portions of atmosphere:

$$DSLF = n\,F_{cloudy}^{\downarrow} + \left(1 - n\right)F_{clear}^{\downarrow} \tag{4}$$

where n is the cloud fraction obtained from visible and infrared imagers.

Table 1 Formulations for effective sky emissivity and temperature, used by different bulk parameterization schemes.

Scheme	ε_{sky}	T_{sky}	Applicability
Prata96 (Prata, 1996)	$1 - \left(1 + \frac{w}{10}\right)\exp\left(-\left(1.2 + 3\frac{w}{10}\right)^{1/2}\right)$	T_o	Clear sky
Dilley&OBrien98 (Dilley and O'Brien, 1998)	$1 - \exp\left(-1.66\tau\right)$ where $\tau = 2.23 - 1.88\left(T_2 / 273\right) + 0.74\left(w / 25\right)^{1/2}$	T_o	Clear sky
Josey&al03 (Josey et al., 2003)	1	$T_o + 10.77n^2 + 2.34n - 18.44 + 0.84\left(4.01 - \Delta Td_o\right)$	All sky

2.2. Calibration of the new DSLF formulation

The calibration of parameters in equations (2) and (3) relies on radiative transfer simulations of downward longwave fluxes at the surface. These simulations are obtained from the MODerate spectral resolution atmospheric TRANSsmittance algorithm (MODTRAN4; Berk et al., 2000) applied to the TIGR-like database (Chevallier et al., 2000). Downward surface radiances at five different zenith angles are then computed for wavelnumbers ranging between 100 and 2500 cm^{-1} at a resolution of 1 cm^{-1}. Such values are then integrated to provide total downward fluxes within the long-wave domain of the spectrum. The model is configured to use ozone and trace gases climatological data of MODTRAN, and the "Rural" aerosol profile. Temperature and humidity, available at 60 vertical levels between the surface and 10 Pa, are obtained

from the TIGR-like dataset. This contains a total of 13495 globally distributed profiles representative of a wide range of atmospheric conditions.

Figure 1 shows MODTRAN estimations of sky emissivity, ε_{sky}, obtained using simulations of DSLF for $F^{\downarrow}$, and 2m temperature as T_{sky}, in equation (1), considering (i) clear sky conditions, i.e., atmospheric profiles where total cloud cover, TCC, equals 0; and (ii) overcast cases, where TCC=1. Given the steep decline of ε_{sky} for very dry atmospheres for overcast, and particularly, for clear sky cases, the calibration of parameters in (2) followed a piecewise regression approach. Each of the clear sky and overcast calibration datasets were then split into three and two (overlapping) classes of TCWV, respectively. For clear sky cases, α and β were adjusted by least squares fitting of (2), with m=0.5, to atmospheric profiles with TCWV $\leq$ 10 mm, and TCWV within the 5-20 mm range and TCWV above 15mm, respectively; the resulting curves intercept at ~2.5mm, and at ~15.5 mm (Figure 1a). For overcast conditions, m was set to 1 and α and β were adjusted to profiles with TCWV $\leq$ 15 mm and TCWV $\geq$ 8 mm, respectively; the resulting curves intercept at ~13mm (Figure 1b). The next step consisted of fitting coefficients γ, and δ in (3) to an optimal T_{sky} obtained by introducing ε_{sky} from (2) in equation (1).
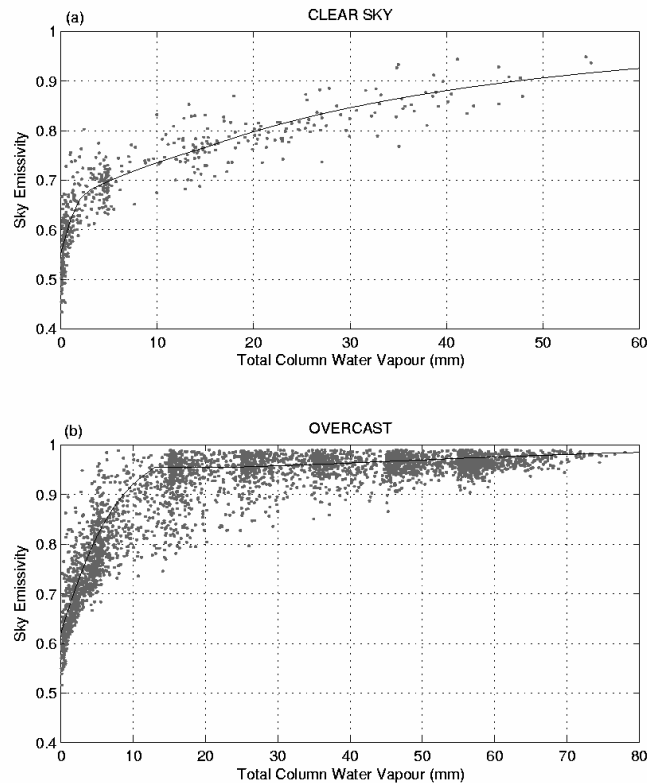

Figure 1 Sky emissivity simulated by MODTRAN (dots) plotted as a function of TCWV for clear sky (top panel) and overcast (lower panel) conditions. The solid line represents the values obtained with equation (2), fitted to MODTRAN estimations.

Figure 2 presents scatterplots of different parameterized DSLF values versus MODTRAN simulations. When compared with the remaining schemes described in Table 1, the new parameterization (equations (2)-(3)) is able to reproduce MODTRAN DSLF, with lower (negligible) bias and root mean square differences (RMSD). Most formulations analysed here for DSLF exhibit conditional biases, i.e., they generally overestimate the lower DSLF values (e.g., Prata96, Dilley&Obrien98, Josey&al03; Figure 2) and/or underestimate those within the higher ranges (Dilley&Obrien98, Josey&al03; Figure 2). Parameterizations of downward long-wave fluxes are often strongly tight to the calibration data. This is clearly the case for the Josey&al03 (Table 1) scheme, which relied on data collected during oceanographic campaigns. Although these observations were taken over a wide latitudinal range, from the subtropics to the Artic (Josey et al., 2003), the formulation is unable to reproduce the extremes of DSLF distribution. These are likely to correspond either to dry and extremely warm, or very dry and cold conditions only likely to be observed inland.
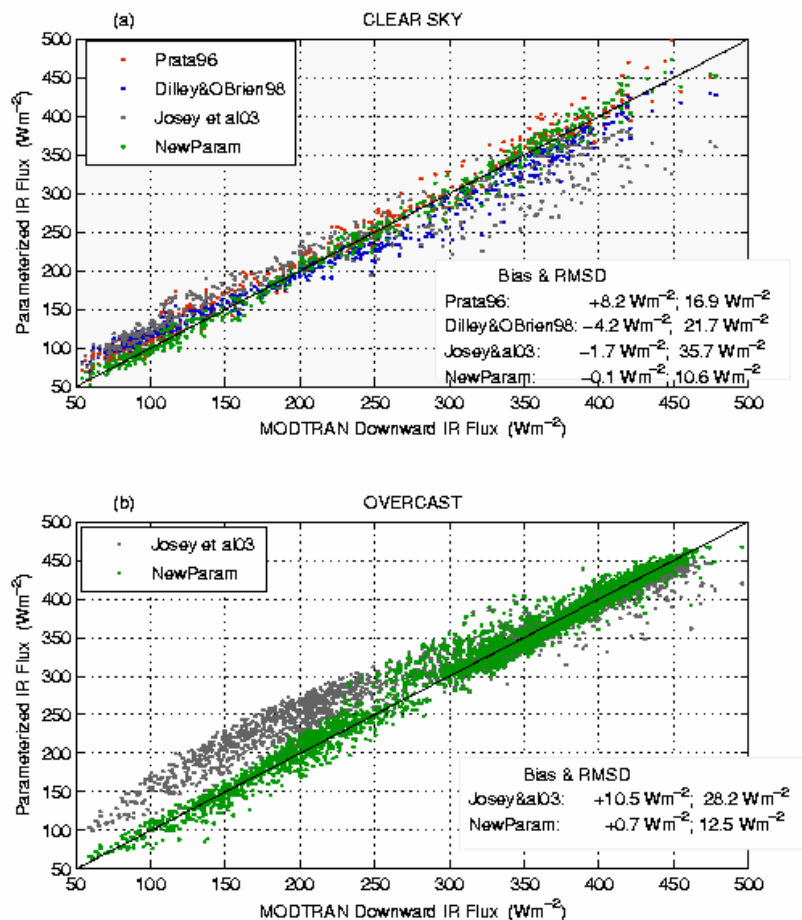
Figure 2 DSLF estimations obtained with different parameterization schemes (dots coloured according to legend) versus MODTRAN simulations (x-axis), for clear sky (upper panel) and

overcast (lower panel) conditions. Systematic differences (parameterizations minus MODTRAN) and root mean square differences are also indicated.

The comparison of different parameterization schemes with MODTRAN simulations does not constitute a proper validation of the former. Moreover, the new version of Prata's formulation was adjusted to the MODTRAN estimations, and thus its better performance when compared with the remaining methodologies was expected. In the next section all schemes will tested against a set of independent data obtained from in situ observations.
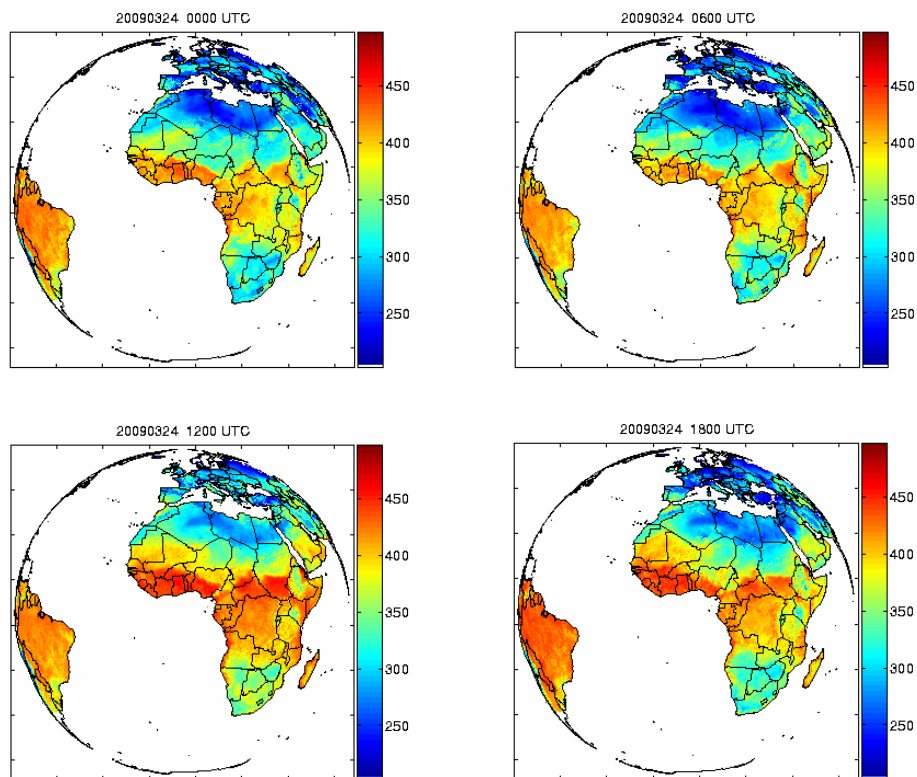
Figure 3 DSLF obtained for 00, 06, 12 and 18 UTC of the 24th March 2009, using the new parameterization scheme. The scene characterization of each SEVIRI pixel (as clear sky or snow, cloud filled, or partially cloudy) was obtained from the NWC SAF software, while ECMWF TCWV, 2m temperature and 2m dew point were bi-linearly interpolated to the Meteosat projection. Temperature and dew point were also corrected, taking into account ECMWF model orography and a digital elevation model, at the SEIVIR spatial resolution.

3. Comparison against In Situ Observations

3.1. Data

DSLF is then estimated using the formulations detailed in Table 1, as well as the new parameterization scheme corresponding to equations (2) to (4), with a 30 minute frequency and for the SEVIRI/Meteosat disk. Atmospheric parameters TCWV, T_o and ΔTd_o are provided by ECMWF 3-hourly forecasts (steps between 12 and 36h), linearly interpolated in time and are bi-linearly interpolated to the projection of SEVIRI level 1.5 data (sampling distance of 3 km at nadir). T_o is corrected for the difference between model orography and the local pixel height, using a constant lapse rate of 0.67K/100m, while ΔTd_o is kept unchanged. The cloud fraction is obtained from the cloud mask developed by Derrien and Gleau (2005) for SEVIRI/Meteosat data, within the context of the NWC SAF. The algorithm is based on a multispectral threshold technique designed to optimize the use of the rich spectral characteristics of SEVIRI (Derrien and Gleau, 2005). The Prata96 and Dilley&Obrien98 schemes (Table 1) are tested for clear sky conditions only, according to the classification provided by the cloud mask. For pixels classified as "totally cloudy" by the NWC SAF cloud mask, n in (3) and in Josey&al03 scheme is assigned to 1, while for "partially cloudy" pixels, n is assigned to 0.5. The time-series of DSLF based on the blending of ECMWF forecasts and satellite clouds, used as input for the various formulations described above, are available since May 2005. Figure 3 shows an example of DSLF fields obtained through the application of the new parameterization scheme to the full Meteosat disk, for the 24th March 2009.

The list of in situ observations used here is detailed in Table 2. Most of these are provided by the Baseline Surface Radiation Network (BSRN; Ohmura *et al*., 1998), while data at Roissy and Carpentras were obtained directly from Météo-France. The choice of ground observations was constraint by area coverage of Meteosat disk and the beginning of DSLF time-series (January 2005). Since most BSRN ground stations are located in Europe, the set is complemented with data collected during 2006 at Niamey (Niger), within the RADAGAST experiment (Slingo et al., 2009).

Table 2 Characteristics of stations with in situ measurements of downward long-wave radiation used in this study.

Station	Latitude & Longitude	Altitude (m)	Network	Data availability
Lerwick	60.13°N; 1.28°W	84	BSRN	May 2005 – Oct 2006
Toravere	58.25°N; 26.46°E	30	BSRN	May 2005 – Dec 2007
Cambourne	50.22°N; 5.32°W	88	BSRN	May 2005 – Oct 2006
Roissy	49.02°N; 2.53°E	110	M-F	Jan 2005 – Dec 2005
Palaiseau	48.71°N; 2.21°E	156	BSRN	May 2005 – Aug 2007
Payerne	46.82°N; 6.94°E	491	BSRN	Jan 2005 – Dec 2007
Carpentras	44.05°N; 5.03°E	100	BSRN	May 2005 – Jun 2006
Sde Boqer	30.91°N; 34.78°E	500	BSRN	Jul 2005 – Dec 2007
Tamanrasset	22.78°N; 5.51°E	1385	BSRN	Jul 2005 – Dec 2007
Niamey	13.48°N; 2.17°E	188	RADAGAST	Jan 2006 – Dec 2006

3.2. Results and Discussion

Figure 4, Figure 5, and Figure 6 present scatter plots of modelled DSLF values, using different formulations and ECMWF model, for 3 stations characteristic of middle latitudes, high latitudes, and arid regions, respectively. These diagrams generally confirm the results obtained with the comparison between parameterization schemes and MODTRAN simulations. Overall, the validation against in situ measurements indicates that the modified version of the algorithm initially proposed by Prata (1996), performs better that the remaining formulations, for both clear and cloudy conditions, proving that the DSLF product can be significantly improved. The absolute biases of ~70-to-80 Wm^{-2} (obtained when the Josey03 formulation is applied) in Tamanrasset for cloudy cases were reduced to less than 10 Wm^{-2}.
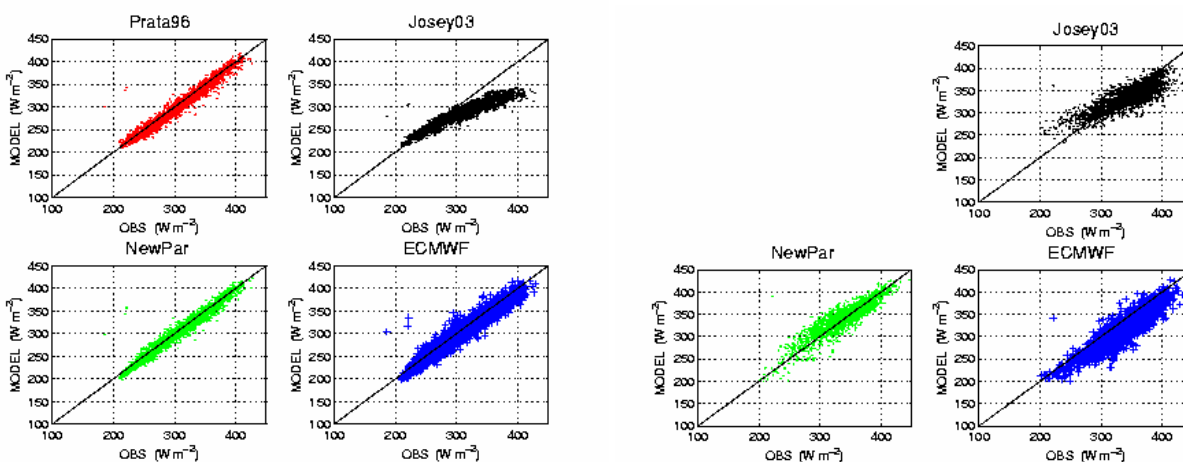

Figure 4 Scatterplots of DSLF (Wm^{-2}) obtained from different parameterization schemes (according to the title of each panel) against in situ measurements taken at Carpentras in France (horizontal axis). Blue crosses: ECMWF downward thermal fluxes at the surface, orographically corrected to the station height. Four left panels correspond to CLEAR SKY cases, while the right panels show the results for 3 models applicable to CLOUDY conditions.

The scatter-plots in Figure 4, Figure 5, and Figure 6 show that dispersion around the 1:1 line is smaller for clear sky cases, than for cloudy conditions, when the thermal radiation reaching the surface depends on factors such as cloud base height and cloud microphysics. Under clear sky conditions, some of the stations show a few points with larger under-estimation of the observations (see Figure 5), which seem to correspond to undetected clouds. Toravere presents a set of such points clearly lying below the 1:1 line, most of which obtained during the winter months, when low solar zenith angles combined with high view angle makes the pixel classification more difficult.
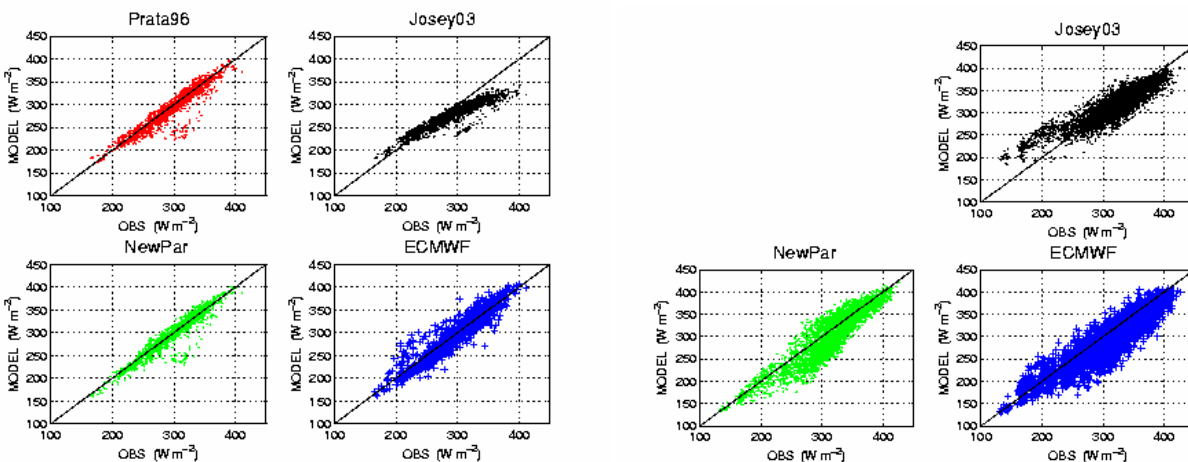
**Figure 5 As in Figure 4, but for Toravere (Estonia).**
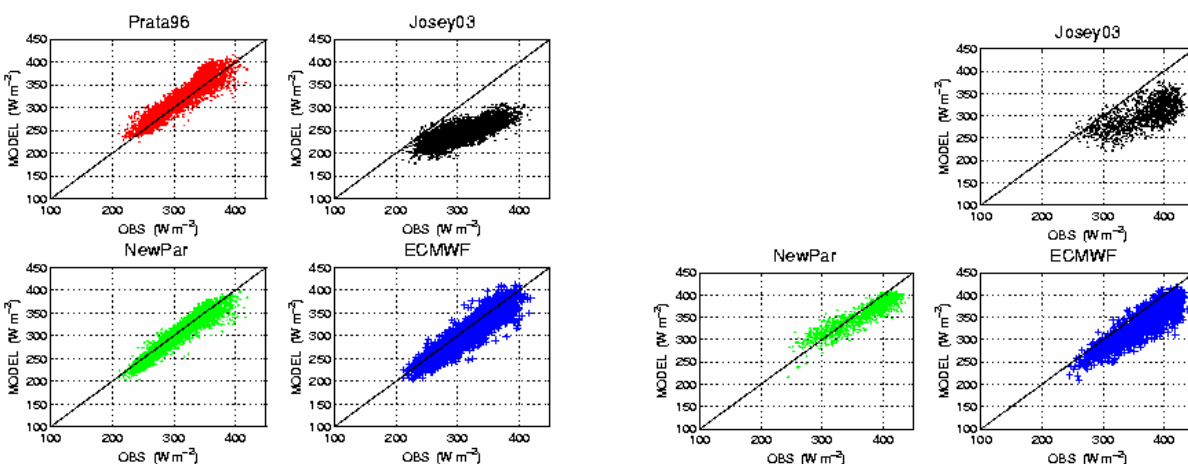
Figure 6 As in Figure 4, but for Tamanrasset (Sahara).

The average differences and RMSE between DSLF estimations and in situ observations are show in Figure 7 and Figure 8, for DJF, MAM, JJA, and SON. Overall, the new parameterization scheme presents systematic errors below 10 Wm^{-2}, with the exception of the cases discussed below. The new scheme also tends to perform better than ECMWF simulations, suggesting that despite its simplicity it partially corrects for deficiencies in ECMWF cloud modelling (e.g., Crewel et al., 2002; Meetschen et al., 2004), benefiting as well of the finer spatial representation of the remote sensing cloud mask. The results obtained using the scheme developed by Josey et al. (2003) are the most variable: DSLF estimations are comparable with those obtained from other schemes in middle-to-high latitude stations, but present strong negative bias during the warm season in Europe, and during all year round in the most southern stations (Sde Boquer in Israel, Tamanrasset in Algeria and Niamey in Niger). The modified version of the Prata formulation for cloudy conditions outcomes Josey03 simulations for most stations. For clear sky conditions, the scores obtained by the original and modified version of Prata's algorithm are fairly similar.
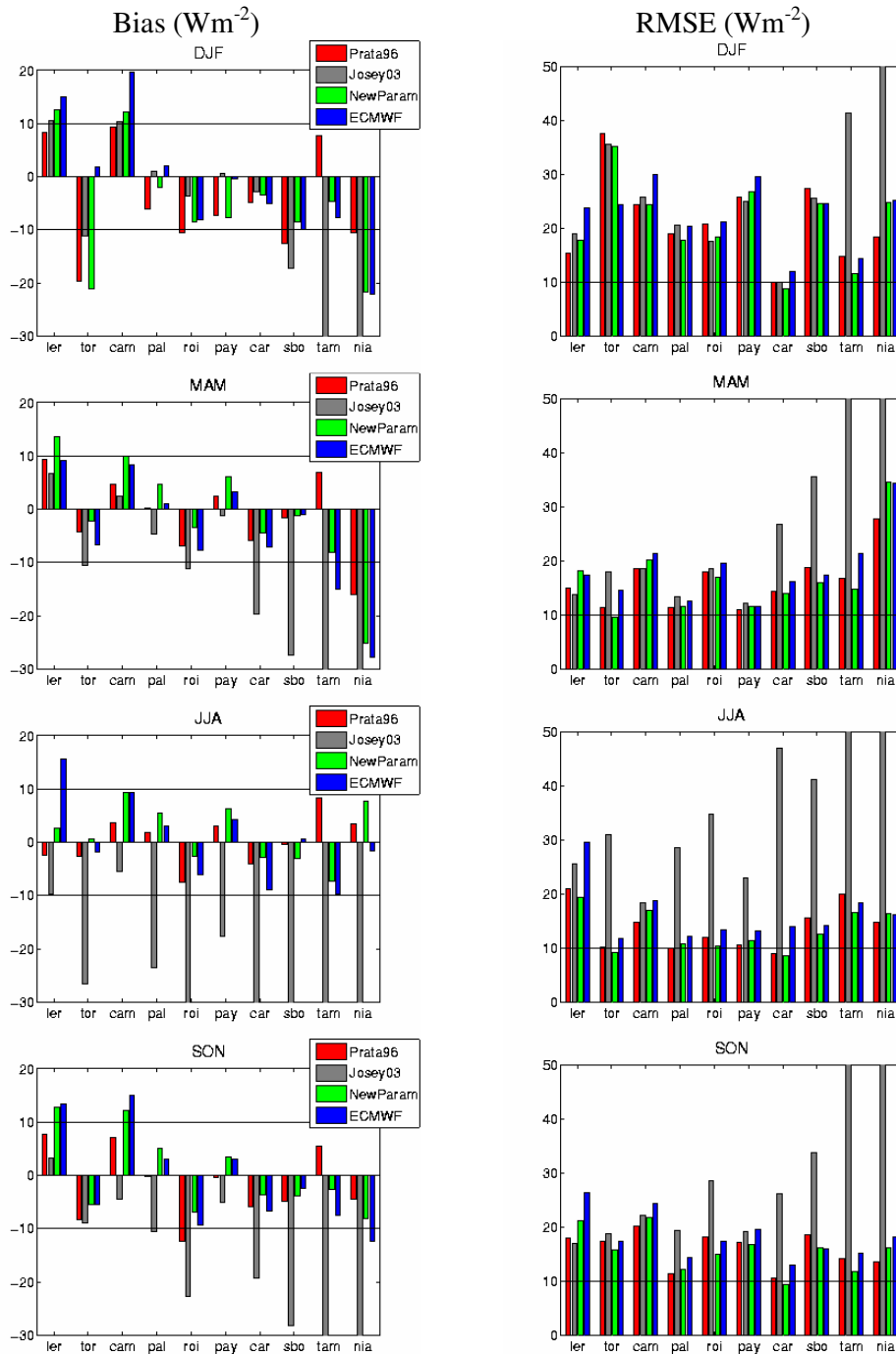
Figure 7 Seasonal bias (left column; Wm-2) root mean square differences (right column; Wm-2) between clear sky DSLF estimations and in situ observations, for the following stations: Lerwick, Toravere, Cambourne, Palaiseau, Roissy, Payerne, Carpentras, Sde Boqer, Tamanrasset, and Niamey. Statistics obtained for Prata96, Josey03, the new scheme, and for ECMWF correspond to red, grey, green, and blue bars, respectively. Please notice that there cases where Josey et al. (2003) bar is truncated, to ensure readability of the remaining elements in the respective diagrams.

Bias (Wm^{-2})   RMSE (Wm^{-2})
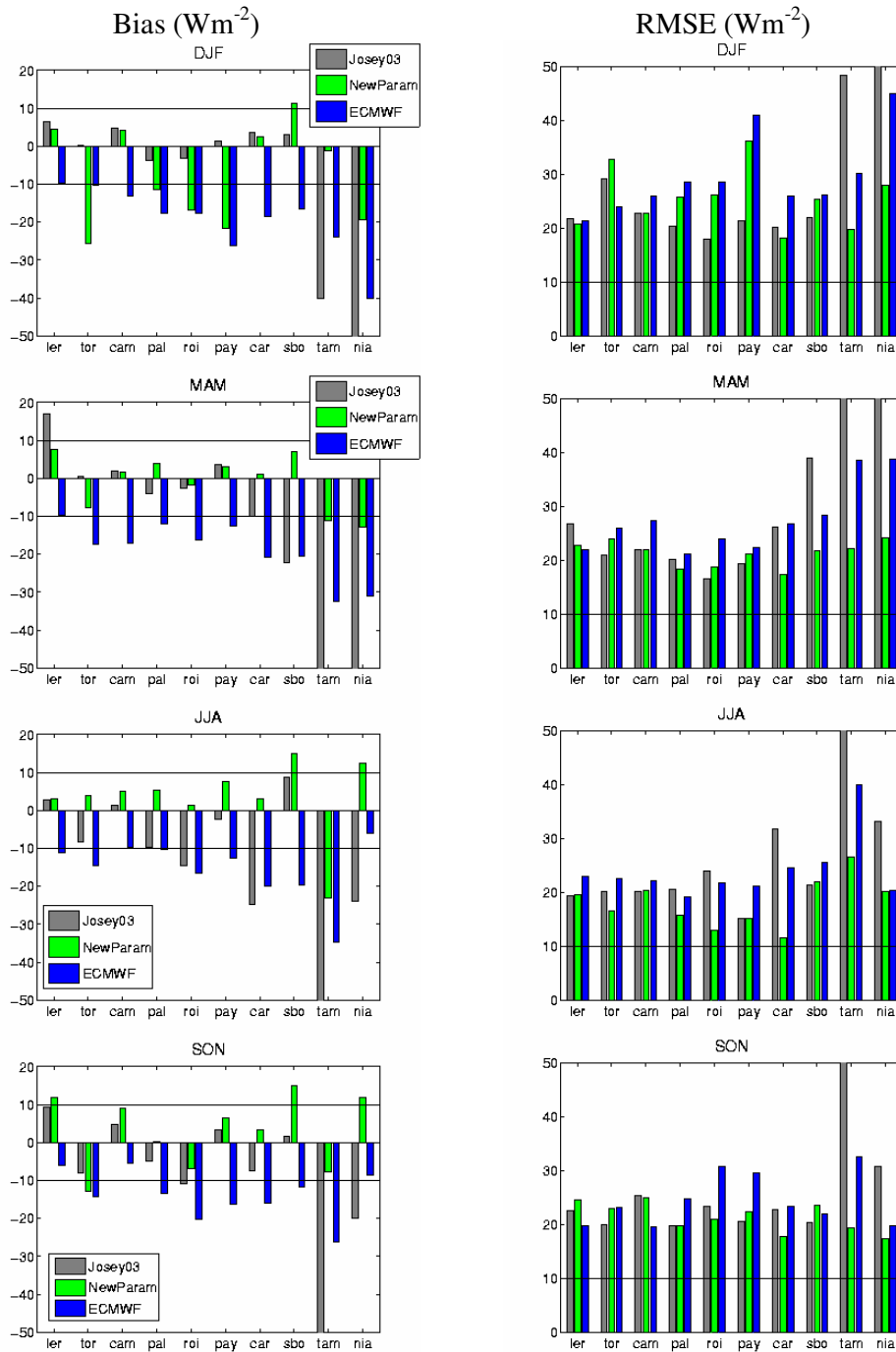
Figure 8 As in Figure 7, but for cloudy (overcast and partially cloudy) cases.

The new parameterization scheme exhibits poorer performances for Toravere during the winter months, where it underestimates local observations by over 20 Wm^{-2}, in both clear and cloudy sky conditions. The clear sky results may be partially explained by an under-classification of cloudy scenes. The cloudy sky scores are not fully

understood. Niamey, particularly during DJF and MAM, is another critical site, where the modified Prata formulation underestimates local observations of clear and cloudy fluxes. The Niamey region was characterized by relatively high aerosol loads, and also suffered severe dust storms in March (Slingo et al., 2006). The parameterization formulations analysed here, and the ECMWF model, were clearly unable to simulate the atmospheric downward fluxes in such extreme conditions.

The parameterization scheme developed for all sky conditions by Josey et al. (2003) performs reasonably well (with biases of 10 Wm^{-2} or less), particularly for stations located in the middle-to-high latitudes during winter. This formulation presents, however, large negative biases when modelling higher DSLF values. This scheme was adjusted to ground data collected during oceanographic campaigns, which took place between the Balearic Islands and Iceland, and has severe limitations in its applicability to in-land regions, particularly under extreme cold/warms and dry conditions.

4. Concluding Remarks

In order to determine an adequate formulation to estimate down-welling surface long-wave fluxes (DSLF), we performed an assessment of different bulk parameterizations, including: (i) two schemes applicable to clear sky conditions developed by Prata (1996), in use by the Land-SAF until 2008; (ii) the scheme first proposed by Josey et al. (2003), applicable to all sky conditions, and in use by the Land-SAF for cloudy cases only until 2008; and (iii) a generalized version of the formulation first proposed by Prata (1996), valid for all sky conditions. The latter was calibrated using data simulated MODTRAN for the TIGR-like database (Chevallier et al., 2001).

The performance of the above-mentioned methods is verified against in situ data collected in several stations in Europe, one in the Middle East, and two in Africa (Table 2). It is shown that the schemes developed by Prata (1996) and its modified version presented here are able to reproduce well the observations for clear sky cases, obtaining often lower biases than ECMWF modelled fluxes. DSLF estimated with those formulations exhibits larger discrepancies with observations taken at Toravere during the winter months. These are likely to be associated to the misclassification of (partially) cloudy pixels as cloud free. Such errors tend to occur for regions with high view angles (as Toravere), being more frequent during night-time when visible channels are not available, or for low solar zenith angles (winter, early morning, or close to sunset). The results obtained for Niamey during the first 6 months of 2006 are also worth noticing. Particularly during February and March, the area was characterized by large aerosol loads and a few events of dust storm (Slingo et al., 2006, 2009), leasing to the underestimation of DSLF by all models analysed here. Josey et al. (2003) presents generally poorer results for clear sky conditions, particularly under warmer conditions.

The comparison between modelled and observed DSLF, for cloudy pixels reveals, as expected, higher error dispersion, than in clear sky conditions. Cloud characteristics, such as cloud base or cloud microphysics play a role in the thermal flux that reaches the surface are very difficult to model or determine from remote sensing data. Nevertheless, the parameterization scheme presents RMSE of the order of 20 Wm^{-2},

for most stations, and, despite its simplicity, performs better that ECMWF in many cases. As mentioned before, Josey et al. (2003) performs well within a relatively narrow set of conditions, limited by the observations used for training obtained in maritime environments.

The study presented here regards the use of cloud information retrieved from SEVIRI/Meteosat to estimate DSLF. A similar methodology may also be applied to AVHRR/MetOp data.

5. References

Berk, A., G.P. Anderson, P.K. Acharya, J.H. Chetwynd, L.S. Bernstein, E.P. Shettle, M.W. Matthew, and S.M. Alder-Golden, 2000: *MODTRAN4 Version 2 User's Manual Air Force Res. Lab*., Space Vehicles Directorate, Air Force Material Command, Hanscom AFB, MA, 2000.

Bilbao, J., and A. H. de Miguel, 2007: Estimation of Daylight Downward Longwave Atmospheric Irradiance under Clear-Sky and All-Sky Conditions. *J. Appl. Meteor. Climatol*., **46**, 878–889. DOI: 10.1175/JAM2503.1

Brunt, D., 1932: Notes on radiation in the atmosphere, I. *Quart. J.Roy. Meteor. Soc*., **58**, 389 – 418.

Brutsaert, W., 1975: On a derivable formula for long-wave radiation from clear skies. *Water Resour. Res*., **11**, 742–744.

Chevallier, F., A. Chédin, F. Chéruy, and J.-J. Morcrette, 2000: TIGR-like atmospheric-profile databases for accurate radiative-flux computation. *Q. J. R. Meteorol. Soc*., **126**, pp. 777-785.

Crawford, T. M, and C. Duchon, 1999: An improved parameterization for estimating effective atmospheric emissivity for use in calculating downwelling longwave radiation. *J. Appl. Meteor*., **38**, 474–480.

Crewell, S., M. Drusch, E. van Meijgaard, and A. van Lammeren, 2002: Cloud observations and modelling within the European BALTEX Cloud Liquid Water network. *Boreal Environ. Res.,* **7,** 235–245.

Derrien, M. and Gléau, H. Le 2005: MSG/SEVIRI cloud mask and type from SAFNWC, *Int. J. Remote Sens*., **26**, 4707 – 4732. doi:10.1080/01431160500166128

Diak, G. R., Bland, W. L., Mecikalski, J. & Anderson, M. C. 2000: Satellite-based estimates of longwave radiation for agricultural applications. *Agric. For. Met*. **82**, 219–226.

Dilley, A.C. and D.M. O'Brien 1998: Estimating downward clear sky long-wave irradiance at the surface from screen temperature and precipitable water, *Q. J. R. Meteorol. Soc*., **124**, 1391-1401.

Dürr, B., and R. Philipona, 2004: Automatic cloud amount detection by surface longwave downward radiation measurements. *J. Geophys. Res*., **109**, D05201, doi:10.1029/2003JD004182

Feijt, A., and P. de Valk, and S. van der Veen, 2000: Cloud detection using Meteosat imagery and numerical weather prediction model data. *J. Appl. Meteor*., **39**, 1017–1030.

Gupta, S. K., 1989: A parameterization for longwave surface radiation from sun-synchronous satellite data. *J. Climate*, **2**, 305-320.

Gupta, S. K., W. L. Darnell, and A. C. Wilber 1989: A parameterization for longwave surface radiation from satellite data: recent improvements. *J. Appl. Meteor*., **31**, 1361-1367.

Idso, S. B., and R. D. Jackson, 1969: Thermal radiation from the atmosphere. *J. Geophys. Res*., **74**, 5397–5403.

Josey, S.A., Pascal, R.W., Taylor, P.K., Yelland, M.J., 2003: A New Formula For Determining the Atmospheric Longwave Flux at Ocean Surface at Mid-High Latitudes. *J Geophys. Res*., doi:10.1029/2002JC00141

Kalma, J. D., T. R. McVicar, and M. F. McCabe, 2008: Estimating land surface evaporation: a review of methods using remotely sensed Surface Temperature Data. *Surv Geophys*, **29**, 421–469, DOI 10.1007/s10712-008-9037-z

Meetschen, D., B. J. J. M. van den Hurk, F. Ament, and M. Drusch, 2004: Optimized Surface Radiation Fields Derived from Meteosat Imagery and a Regional Atmospheric Model. *J. Hydrometeor*., **5**, 1091-1101.

Morcrette, J.-J., 2002: Assessment of the ECMWF model cloudiness and surface radiation fields at the ARMSGP site. *Mon. Wea. Rev*.,

Niemelä, S., P. Räisänen, and H. Savijärvi, 2004: Comparison of surface radiative flux parameterizations part I: Longwave radiation. *Atmos. Res*., **58**, 1-18.

Ohmura A., Dutton, E.G., B. Forgan, C. Fröhlich, H. Gilgen, H. Hegner, A. Heimo, G. König-Langlo, B. McArthur, G. Müller, R. Philipona, R. Pinker, C. H. Whitlock, K. Dehne, and M. Wild. 1998: Baseline Surface Radiation Network (BSRN/WRMC), a new precision radiometry for climate research. *Bull. Amer. Meteor. Soc*., **79**, 2115 - 2136

Prata, A.J., 1996: A new long-wave formula for estimating downward clear-sky radiation at the surface, *Q. J. R. Meteorol. Soc*., **122**, 1121-1151.

Rossow, W. B., and L. C. Garder, 1993: Cloud detection using satellite measurements of infrared and visible radiances for ISCCP. *J. Climate*, **6**, 2341–2369.

Slingo, A. , T. P. Ackerman, R. P. Allan, E. I. Kassianov, S. A. McFarlane, G. J. Robinson, J. C. Barnard, M. A. Miller, J. E. Harries, J. E. Russell, and S. Dewitte, 2006: Observations of the impact of a major Saharan dust storm on the atmospheric radiation balance, *Geophys Res Lett*., **33**, **L24817**, doi:10.1029/2006GL027869.

Slingo, A., H. E. White, N. A. Bharmal, and G. J. Robinson, 2009: Overview of observations from the RADAGAST experiment in Niamey, Niger: 2. Radiative fluxes and divergences, *J. Geophys. Res.*, **114**, **D00E04**, doi: 10.1029/2008JD010497.

Takara, E. E., and R. G., Ellingson, 2000: Broken Cloud Field Longwave-Scattering Effects. *J. Atmos Sci*., **57**, 1298-1310.

Wild, M., A. Ohmura, H. Gilgen, and E. Roeckner 1995: Validation of general circulation model radiative fluxes using surface observations. *J. Clim*., **8**, 1309-1324.

Zhang, Y.-C., W. B. Rossow, and A. A. Lacis 1995: Calculation of surface and top of atmosphere radiative fluxes from physical quantities based on ISCCP data sets: 1. Method and sensitivity to input data uncertainties, *J. Geophys. Res*., **100**, 1149–1165.

Zhao, W., W. R. Kuhn, and S. R. Drayson, 1994: The significance of detailed structure in the boundary layer to thermal radiation at the surface in climate models. *Geophys, Res. Lett*., **21**, 1631-1634.